European Radiology (2019) 29:153–160
https://doi.org/10.1007/s00330-018-5603-z

COMPUTED TOMOGRAPHY

Improved display of cervical intervertebral discs on water (iodine) images: incidental findings from single-source dual-energy CT angiography of head and neck arteries

Qingxia Wu[1] · Dapeng Shi[1] · Tianming Cheng[1] · Hongming Liu[1] · Niuniu Hu[1] · Xiaowan Chang[2] · Ying Guo[1] · Meiyun Wang[1]

Received: 15 March 2018 / Revised: 28 May 2018 / Accepted: 7 June 2018 / Published online: 19 June 2018

Abstract

Objective To (a) assess the diagnostic performance of material decomposition (MD) water (iodine) images for the evaluation of cervical intervertebral discs (IVDs) in patients who underwent dual-energy head and neck CT angiography (HNCTA) compared with 70-keV images and (b) to explore the correlation of water concentration with the T2 relaxation time of IVDs.

Materials and methods Twenty-four consecutive patients who underwent dual-energy HNCTA and cervical spine MRI were studied. The diagnostic performance of water (iodine), 70-keV and MR images for IVD bulge and herniation was assessed. A subjective image score for each image set was recorded. The signal-to-noise ratio (SNR) and contrast-to-noise ratio (CNR) of IVDs to the cervical spinal cord were compared between water (iodine) and 70-keV images. Disc water concentration as measured on water (iodine) images was correlated with T2 relaxation time.

Results IVD evaluations for bulge and herniation did not differ significantly among the three image sets (pairwise comparisons; all $p > 0.05$). SNR and CNR were significantly improved on water (iodine) images compared with those on 70-keV images ($p < 0.001$). Although water (iodine) images showed higher image quality scores when evaluating IVDs compared with 70-keV images, the difference is not significant (all adjusted $p > 0.05$). IVD water concentration exhibited no correlation with relative T2 relaxation time (all $p > 0.05$).

Conclusion Water (iodine) images facilitated analysis of cervical IVDs by providing higher SNR and CNR compared with 70-keV images. The disc water concentration measured on water (iodine) images exhibited no correlation with relative T2 relaxation time.

Key Points

- *There was no significant difference in cervical IVD evaluations for bulge and herniation among water (iodine) images, 70-keV images and MR images.*
- *Water (iodine) images provided higher objective and subjective image quality than 70-keV images, though the difference of subjective evaluation was not statistically significant.*
- *The disc water concentration exhibited no correlation with relative T2 relaxation time, which reflects the inferiority of the water (iodine) images in evaluating disc water content compared with T2 maps.*

Electronic supplementary material The online version of this article (https://doi.org/10.1007/s00330-018-5603-z) contains supplementary material, which is available to authorized users.

✉ Meiyun Wang
mywang@ha.edu.cn

[1] Department of Radiology, Henan Provincial People's Hospital, No. 7 Weiwu Road, Zhengzhou 450003, Henan, China

[2] Department of Operation and Management, Henan Provincial People's Hospital, No. 7 Weiwu Road, Zhengzhou 450003, Henan, China

Keywords Intervertebral disc · Dual-energy scanned projection radiography · Computed tomography angiography · Image quality enhancement · Magnetic resonance imaging

Abbreviations

ASIR-V	Adaptive statistical iterative reconstruction V
CNR	Contrast-to-noise ratio
CTA	Computed tomography angiography
DECT	Dual-energy computed tomography
DLP	Dose-length product
FSE	Fast spin echo
GSI	Gemstone spectral imaging
HAP	Hydroxyapatite
HNCTA	Head and neck computed tomography angiography
IVD	Intervertebral disc
MD	Material decomposition
ROI	Region of interest
SFOV	Scan field of view
SNR	Signal-to-noise ratio

Introduction

Dual-energy CT (DECT) with virtual monochromatic images has shown promise for iodine load, injection rate and radiation dosage reduction in the application of pulmonary, renal, upper and lower extremity, and head and neck CT angiography (HNCTA) [1–5].

The cervical vertebrae and intervertebral discs (IVDs) frequently require evaluation during HNCTA because disc degeneration can produce symptoms similar to those of cerebral ischaemia, such as headache, fatigue and vertigo [6–8]. However, conventional CT is inferior to MRI for the evaluation of disc degeneration because of the low soft-tissue contrast and subjectivity to beam hardening and motion movement artefacts. MRI is the modality of choice for assessing IVD. T1- and T2-weighted MRI help classify IVD degeneration using the Pfirrmann and Modic grading systems [9, 10]. Moreover, T2 relaxation time reflect the water content of IVDs [11, 12].

The material decomposition (MD) technique of DECT allows the decomposition of a mixture of two or more different elemental composition into its constituent materials, such as iodine, water, calcium and hydroxyapatite (HAP), resulting in various MD images such as water (iodine), iodine (water), water (calcium) and calcium (water) images, which can help to differentiate and quantify tissue types and material concentrations [13]. We observe that the nucleus pulposus of the disc, a highly hydrated structure, manifests as an area of relatively high signal intensity on MD water (iodine) images, indicating that DECT may have great potential in IVD analysis, not only for the IVD morphology display, but also for evaluation of disc degeneration. To the best of our knowledge, no studies have been performed on cervical IVDs by using a MD technique. Therefore, the aims of this study were to evaluate if water (iodine) images from patients who underwent dual-energy HNCTA would allow improved analysis of IVDs compared with 70-keV images and disc water concentration as measured on water (iodine) images could reflect the water content of IVDs and show correlation with T2 relaxation time.

Materials and methods

Study population

Our prospective study was approved by the institutional review board and written informed consent was obtained from all patients who underwent HNCTA prior to study inclusion, and an additional cervical spine MRI was taken for each of them.

From November 2017 and January 2018, 24 consecutive patients with neurological symptoms who had been referred for HNCTA were prospectively enrolled. There were 16 men and 8 women who ranged in age from 27 to 70 years (mean age, 51.8 ±10.7 years). All the patients underwent cervical spine MRI 2 to 7 hours after HNCTA on the same day.

Dual-energy HNCTA protocol

Dual-energy HNCTA images were acquired with a 16-cm-wide detector CT scanner (Revolution CT, GE Healthcare). Each patient was scanned in the supine position with the gemstone spectral imaging (GSI) mode. The scan parameters are listed in Table 1. After scout CT scanning, each patient was

Table 1 Scan parameters for the dual-energy head and neck CT angiography (DEHNCTA) protocol

DEHNCTA	
Mode	GSI helical
Rotation speed (s/rot)	0.5 s/rot
Pitch	0.992:1
Tube voltage (KVp)	80/140 KVp
Tube current (mA)*	Dose modulation with noise index 5
Beam collimation	128 × 0.625
SFOV	50.0 cm
ASIR-V	50%

Note: * Automatic exposure control on. SFOV: Scan field of view. ASIR-V: Adaptive statistical iterative reconstruction V

injected with non-ionic contrast material (Ultravist 370, Bayer Healthcare) through the right antecubital vein to avoid severe reflux. The contrast medium dose was 45–50 mL delivered at a rate of 4–4.5 mL/sec. The injection was performed with a power injector (Missouri-XD2001; Ulrich Medical). Automated scan triggering software (SmartPrep; GE Healthcare) was employed to determine the scanning delay. A region of interest (ROI) was placed on the descending aorta to monitor the contrast medium. The scanning delay was set as the time at which the CT value of the aorta ROI reached the threshold level of 160 Hounsfield units (HU) plus 2 seconds. The scan range was from the aortic arch to the top of the head.

We selected 70-keV images for comparison with water (iodine) images because previous studies have demonstrated that energy levels between 60 and 77 keV are effective for soft tissue evaluation, and 70-keV has been used extensively for clinical diagnoses [14, 15]. Two image sets of 70-keV and water (iodine) images with section thicknesses of 1.25 mm were reconstructed and transmitted to an offline workstation (Advantage Workstation 4.7; GE Healthcare). GSI Volume Viewer was employed to generate sagittal and axial water (iodine) images for the evaluation of cervical IVDs.

MRI protocol

Spine MRI of all subjects were obtained with a 3-T MR imager (Magnetom Skyra; Siemens Healthineers) equipped with a dedicated 20-channel head and neck coil. The scan sequences and parameters are listed in Table 2.

Subjective image analysis

Two radiologists (with 7 and 23 years of experience in musculoskeletal radiology) analysed the water (iodine) images, 70-keV images and MRI images together in a randomised fashion. All three image sets were reviewed on an AW4.7 workstation. The water (iodine) images and 70-keV images had section thicknesses of 1.25 mm and were reconstructed in sagittal and coronal orientations that were linked with transverse lines. Partial annotations were obscured to ensure blindness during the subjective evaluation of water (iodine) images and 70-keV images. The time interval of the evaluation of each image set was one week.

Visual analysis

Both readers evaluated each IVD from C2–C7 of each patient on the three image sets. The visual morphological evaluations of all IVDs were performed based on sagittal and axial images. Discs were graded based on the morphologies of their posterior, posterior lateral, anterior and far lateral aspects in terms of focal disc herniation (protrusion or extrusion), disc bulging or the absence of such abnormalities, which indicated normal discs [16–18].

The subjective image quality based on the conspicuity of IVDs and image noise was assessed using a five-point scale (1 = major artefact rendering poor opacification of the IVD and a nondiagnostic image, 2 = major artefact with suboptimal opacification of the IVD and low diagnostic confidence, 3 = moderate artefact with limited opacification of the IVD but image quality sufficient for diagnosis, 4 = minor artefact with good opacification of the IVD and no influence on diagnosis, 5 = no perceivable artefact with excellent opacification of the IVD). The scoring system is described in CT pulmonary angiography studies by Schueller-Weidekamm et al [19] and Yuan et al [1]. When the two observers disagreed on the morphologies and image scores of IVDs, consensus was reached by discussion. Adjustments of window level and width were allowed during qualitative assessment. The five-point scale was used to evaluate each segment of one patient and then compared.

Objective image analysis

Readers 1 and 2 performed quantitative image analyses independently after subjective analyses.

Table 2 MR scan parameters for cervical vertebral imaging

MR	T1 FSE sagittal	T2 FSE sagittal	T2 FSE FS sagittal	T2 FSE axial	T2 map sagittal
Repetition time (ms)	650	3770	4000	4000	1100
Echo time (ms)	10	97	88	104	13.8, 27.6, 41.4, 55.2, 69.0
Field of view (mm^2)	270 × 270	270 × 270	270 × 270	240 × 240	270 × 270
Voxel size (mm^3)	0.7 × 0.7 × 3.0	0.7 × 0.7 × 3.0	0.7 × 0.7 × 3.0	0.4 × 0.4 × 3.0	0.7 × 0.7 × 3.0
Slice thickness (mm)	3	3	3	3	3
Interslice gap (mm)	0.6	0.6	0.6	0.6	0.6
Number of slices	11	11	11	3 × 5	11
Acquisition time (min:sec)	1:41	1:38	1:56	1:36	3:40

Note: FSE: fast spin echo

The signal-to-noise ratio (SNR) and contrast-to-noise ratio (CNR)

We measured CT number, water concentration and noise (standard deviation of CT number or water concentration) of each IVD on 70-keV and water (iodine) images. ROIs were placed on the central region of the disc to reflect the signal of the nucleus pulposus and to avoid a partial volume effect of adjacent bone, as were shown in Fig. 1. Then, ROIs were automatically copied to water (iodine) images at the same sagittal position, and water concentration and noise were measured. Another ROI with the same area as that on IVDs was placed on the suboccipital muscle to measure the background noise. SNR was calculated as follows: SNR = SIdisc/noise, where SI = signal intensity. CNR represents the difference in SI between the disc and the cervical spinal cord of the corresponding level. CNR was calculated as follows: CNR = (SIdisc – SIspinal cord)/noise of the suboccipital muscle. SIdisc represents the CT number or water concentration of IVDs and SIspinal cord represents the CT number or water concentration of the spinal cord of the corresponding level.

T2 relaxation time of IVDs

ROIs were placed on each IVD at the central sagittal position of the T2 map. T2 relaxation times were then collected.

Statistical analysis

All statistical analyses were performed with SPSS software (version 22.0; SPSS, IBM). All numerical values are reported as the means ±standard deviation. The Kolmogorov–Smirnov test was performed to test for normal distributions before further statistical analyses. For analysis of the subjective data, IVD evaluations were compared among the three image sets by using the McNemar–Bowker test. For the pairwise comparisons among the three image sets, the α is corrected according to the formula:

$$\alpha' = \frac{\alpha}{\frac{k(k-1)}{2}+1}$$

In our case, the exploited $\alpha' = \frac{0.05}{\frac{3(3-1)}{2}+1} = 0.0125$. Image quality scores were compared among the image sets and the five segments by using the Friedman test; for the following

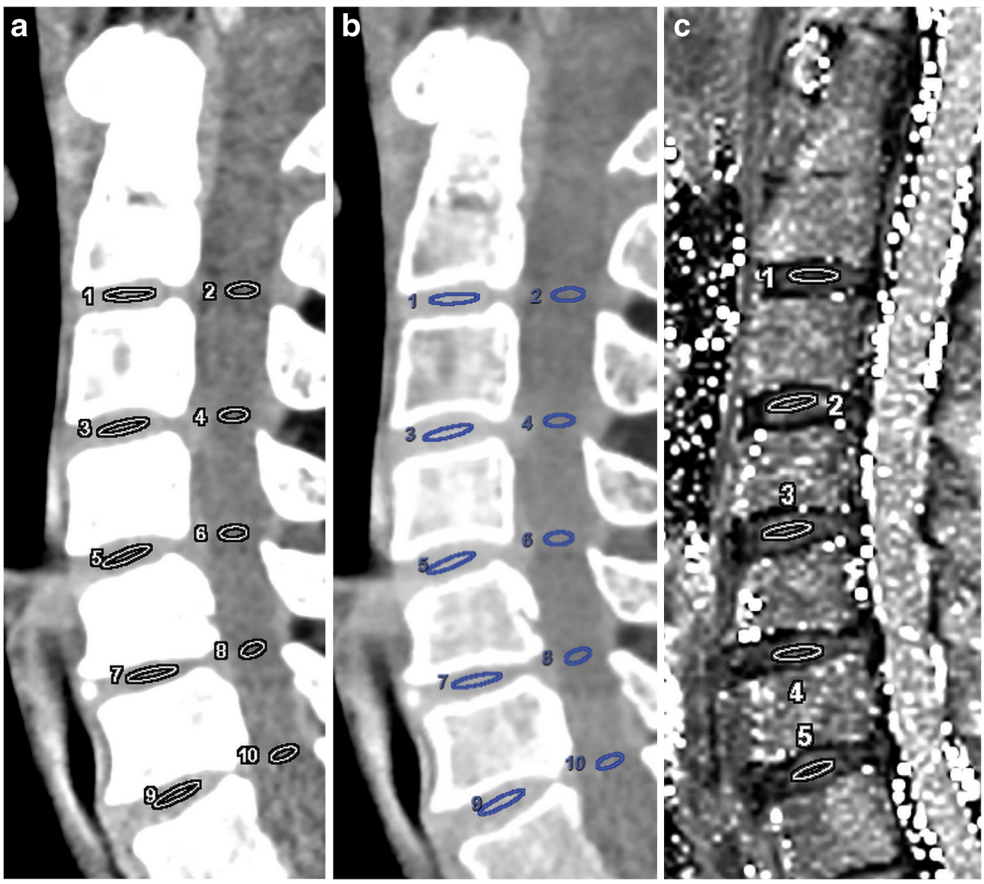

Fig. 1 Images from a 54-year-old woman who underwent head and neck CTA. **a** and **b** show where ROIs were placed on each IVD and spinal cord at the corresponding level on sagittal 70-keV and water (iodine) images, respectively. **c**, Sagittal T2 map; ROIs were placed on IVDs to acquire T2 relaxation times

Table 3 Evaluations of cervical IVDs among the three image sets

IVDs	Water (iodine) images	70-keV images	MR images	*p* value (water vs. 70)	*p* value (water vs. MRI)	*p* value (70 vs. MRI)
Normal	18	18	24	0.317	0.200	0.245
Bulging	24	23	13			
Herniation	70	71	75			

Note: data are numbers of IVDs

pairwise comparison, the significance of difference was determined by the adjusted *p* values provided by SPSS software to rule out pseudo-positive errors. For analysis of objective data, the mean SNR, CNR and T2 relaxation time from the two readers were used. The mean SNR and CNR were compared between water (iodine) and 70-keV image sets by using a paired *t* test. The mean SNRs and CNRs of five IVDs from the same subjects were compared using the Friedman test. Pearson correlation was employed to evaluate correlations of both water concentration and CT number with T2 relaxation time of the IVDs. The interobserver agreement for IVD evaluations was analysed with the weighted κ value, and the agreement for image quality score and each of the objective measures was assessed with the intraclass correlation coefficient. Weighted κ values and intraclass correlation coefficients were interpreted as previously suggested: less than 0.20, poor agreement; 0.21–0.40, fair agreement; 0.41–0.60, moderate agreement; 0.61–0.80, good agreement; and 0.80–1.00, excellent agreement [20].

Results

The mean CT dose index volume of all the subjects' examinations was 11.5 ± 1.2 mGy. The mean dose-length product (DLP) was 471.1 ± 82.2 mGy*cm.

A total of 119 IVDs were assessed in the 24 patients. One C6/7 IVD was not evaluable due to vertebral block. In addition, seven IVDs from three subjects, including one C4/5 IVD, three C5/6 IVDs and three C6/7 IVDs, were excluded due to serious artefacts. The T2 map of one subject was excluded because of poor image quality resulting from a motion artefact.

Subjective image analysis

Of the 112 included discs, 18, 18 and 24 were visually classified as 'normal' for water (iodine), 70-keV and MRI image sets, respectively; 24, 23 and 13 showed bulging for water (iodine), 70-keV and MRI image sets, respectively; and 70, 71 and 75 discs showed herniation as evaluated on water (iodine), 70-keV and MRI image sets, respectively. The McNemar–Bowker test revealed no significant differences in IVD evaluation among the three image sets, all *p* values > 0.0125 (α was set to 0.0125), as shown in Table 3. The mean image scores of C2/3, C3/4, C4/5, C5/6 and C6/7 were 3.30, 3.80, 4.10, 3.95 and 3.05; 3.15, 3.45, 3.70, 3.40 and 2.60; and 4.45, 4.15, 4.20, 3.80 and 4.10 for water (iodine), 70-keV and MRI sets, respectively. Image quality showed no difference for the evaluation of C5/6 IVD ($p = 0.063$). MRI showed significantly improved image quality compared with 70-keV images when evaluating C2/3, C3/4 and C6/7 IVDs, and with water (iodine) images when evaluating the IVD of C2/3 (all adjusted $p < 0.05$). However, although water (iodine) images showed higher image quality scores, the difference was not significant, as shown in Table 4. As for the comparison among the five segments of IVD, C4/5 showed better image quality than C2/3 and C6/7 on water (iodine) images (adjusted $p = 0.023$ and 0.016); C4/5 showed better image quality than C6/7 on 70-keV images (adjusted $p = 0.002$); although there was statistical difference on image quality among the five segments on MRI, the multiple pairwise comparisons were not significant (all adjusted $p > 0.05$).

Table 4 Evaluations of image quality among the three image sets

Image quality	Water (iodine) images	70-keV images	MR images	*p* value	*p* value (water vs. 70)	*p* value (water vs. MRI)	*p* value (70 vs. MRI)
C2/3	3.30 ± 0.733	3.15 ± 0.671	4.45 ± 0.510	0.000*	1.000	0.000*	0.000*
C3/4	3.80 ± 0.768	3.45 ± 0.686	4.15 ± 0.489	0.000*	0.337	0.337	0.004*
C4/5	4.10 ± 0.718	3.70 ± 0.733	4.20 ± 0.696	0.012*	0.166	1.000	0.067
C5/6	3.95 ± 0.759	3.40 ± 0.681	3.80 ± 0.523	0.063	--	--	--
C6/7	3.05 ± 1.191	2.60 ± 0.940	4.10 ± 0.553	0.000*	0.246	0.081	0.000*
p value	0.000*	0.000*	0.006*				

Note: data are the means ± standard deviations; *$p < 0.01$. For the pairwise comparison of image quality, the *p* values provided on the above are the *p* values adjusted by SPSS software directly

Table 5 The mean SNR, CNR and T2 relaxation time of each IVD on water (iodine) images and 70-keV images

	C2/3	C3/4	C4/5	C5/6	C6/7	*p* value
SNR						
Water (iodine) images	166.0 ± 51.6	212.0 ± 80.9	180.2 ± 72.5	188.2 ± 118.1	142.8 ± 60.2	0.061
70-keV images	8.7 ± 2.7	11.2 ± 4.3	9.0 ± 3.4	9.1 ± 4.1	8.1 ± 2.8	0.211
p value	0.000*	0.000*	0.000*	0.000*	0.000*	
CNR						
Water (iodine) images	16.4 ± 5.4	14.6 ± 4.0	14.2 ± 3.9	14.0 ± 4.9	15.6 ± 6.5	0.208
70-keV images	9.4 ± 3.1	8.8 ± 2.6	9.0 ± 2.8	8.4 ± 2.7	10.3 ± 4.8	0.129
p value	0.000*	0.000*	0.000*	0.000*	0.000*	
T2 relaxation time (ms)						
T2 map	56.3 ± 18.2	50.5 ± 11.3	51.7 ± 12.4	51.7 ± 16.6	58.9 ± 23.8	0.416

Note: data are the means ± standard deviations, *$p < 0.01$

The weighted κ value for interobserver agreement on IVD evaluation was 0.953, and the intraclass correlation coefficients for image quality score and objective measures were 0.965 and 1.00, respectively. These values all indicated excellent agreement.

Objective image analysis

SNR and CNR of IVDs

The mean area of ROIs used for quantitative analysis was 10.99 ±3.14 mm^2. The SNR and CNR of the C2–7 IVDs were significantly higher on water (iodine) images than on 70-keV images ($p < 0.05$), as presented in Table 5 and Fig. 2.

The SNR and CNR of each IVD showed no significant difference on either water (iodine) images or 70-keV images ($p > 0.05$).

T2 relaxation Time of IVDs

The mean T2 relaxation time of each IVD from C2–C7 is listed in Table 5. There was no significant difference among IVDs ($p = 0.416$).

Correlations of water concentration and CT number with T2 relaxation time of IVDs

Correlations were found between the CT number and T2 relaxation time of C4/5 (r = –0.474, $p = 0.022$). No other correlations between CT number and water concentration with relative T2 relaxation time were observed, as shown in Table S6.

Discussion

In this study, we explored the potential clinical application of MD water (iodine) images for IVD analysis in HNCTA examinations. The results revealed that water (iodine) images showed accurate IVD status as with MR images and 70-keV images and resulted in improved SNR and CNR values compared with the 70-keV images, which would facilitate the estimation of IVD status in clinical experience.

In subjective visual image assessment analysis, IVD evaluations for bulge and herniation did not differ among the three image sets. As we expected, MR images exhibited best image quality for the evaluation of IVDs. Although the difference is not significant, water (iodine) images showed higher image

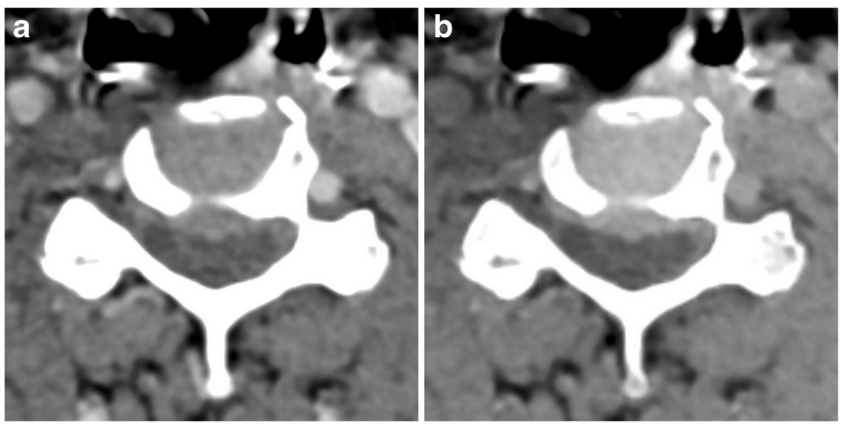

Fig. 2 Images from a 51-year-old man who underwent head and neck CTA. A herniation of C4/5 IVD is shown. **a**, axial 70-keV image, **b**, axial water (iodine) image. **b** shows improved IVD contrast compared with that of **a**

quality scores when evaluating IVDs compared with 70-keV images. This improvement in water (iodine) images over 70-keV images was due to significant increases in the SNR and CNR of IVDs in water (iodine) images, as demonstrated in objective analysis. Due to the high water content of the nucleus pulposus, the discs exhibited higher signal on water (iodine) images and bulging and protrusion could thus be easily identified. Iodine (water) images are frequently used for the precise evaluation of lesion enhancement in various organs and water (iodine) images are often used as virtual non-contrast images [20, 21]. Our results illustrated that the application of water (iodine) images from dual-energy HNCTA examinations for the evaluation of cervical IVDs is promising.

The nucleus pulposus of the IVD is composed mainly of high-molecular-weight glycosaminoglycans with fixed negative charges that induce osmotic swelling [22, 23]. The reported water content of human IVDs ranges from 60 to 80%, with higher water contents in the nucleus pulposus [11]. T2 relaxation time has been demonstrated to exhibit an excellent correlation with water content [24]. However, in our study, water concentrations of the IVDs exhibited no statistical correlation with the corresponding T2 relaxation times, which conflicts with our hypothesis. Possible explanations for this finding include the following: first, the attenuation of IVD on CT images is mainly determined by collagens rather than water, while T2 relaxation time in MRI images is mainly reflecting the amount of water in disks. Thus, the water (iodine) images show inferior capability in evaluating disc water content compared with T2 maps. Second, T2 relaxation time is the decay constant for T2 signal intensity and can be deemed as an intrinsic property of the IVD that reflects the molecular environment created in the disc by water, proteins, collagen and other solutes. Although T2 relaxation times of both the nucleus pulposus and annulus fibrosus correlate well with water content, they vary with age, degeneration stage and duration of compression [11, 25]. The interactions among these parameters are very complicated and there is no simple relationship of T2 relaxation time with any single tissue parameter, as with water concentration measured on the water (iodine) images. Third, the ROIs drawn on the water (iodine) images were not identical to those drawn on T2 maps. And fourth, the number of patients recruited in our study was small, and correlations of water concentration on water (iodine) images with T2 relaxation time and water content need to be verified in large-scale studies.

Our study has several limitations. First, our study mainly focused on the display of IVDs, and vertebral bones, intervertebral joints, radicular canals, spinal cord, paravertebral ligaments and muscles were not evaluated. Second, although noise (standard deviation) has been employed to assess objective image quality in many previous studies, SNR and CNR were chosen to reflect objective image quality because standard deviations for water (iodine) and 70-keV images were in different units and thus could not be directly compared. Third, ROIs of the discs were used for analysis rather than delineating disc margins and generating the whole disc volume, which might not have fully reflected water concentration and T2 relaxation time. ROIs on water (iodine) images were copied to 70-keV images and were thus in the same position, whereas ROIs on T2 maps were drawn independently, which might have led to position bias. ROIs were placed on the nucleus pulposus, which is easily identified on MR images, whereas it is difficult to delineate on CT images; although the ROI was placed in the central of IVD, the error exists inevitably. Fourth, the small number of recruited subjects limits the generalizability of our results. Fifth, although we hid partial annotations for evaluations of IVDs and image quality, the readers were not completely blinded because of the intrinsic features of water (iodine) images and 70-keV images.

In conclusion, water (iodine) images evaluated IVD status accurately as with MR images and resulted in improved SNR and CNR values compared with the 70-keV images, which would facilitate the estimation of IVD status in clinical experience. However, no correlation between disc water concentration and relative T2 relaxation time reflected the inferiority of the water (iodine) images in evaluating disc water content compared with T2 maps.

Funding This study has received funding by the National Key R&D Program of China (YS2017YFGH000397), National Natural Science Foundation of China (81641168, 31470047, 81720108021, 81271565), Henan Province Scientific and Technological Innovation Talents Project (164200510014), Henan Province Scientific and Technological Cooperation Project (152106000014) and Key Project of Henan Medical Science and Technology Project (201501011).

Compliance with ethical standards

Guarantor The scientific guarantor of this publication is Meiyun Wang.

Conflict of interest The authors of this manuscript declare no relationships with any companies, whose products or services may be related to the subject matter of the article.

Statistics and biometry One of the authors, Xiaowan Chang, has significant statistical expertise.

Informed consent Written informed consent was obtained from all the patients prior to study inclusion.

Ethical approval Institutional review board approval was obtained.

Methodology
- prospective
- diagnostic study/observational
- performed at one institution

References

1. Yuan R, Shuman WP, Earls JP et al (2012) Reduced iodine load at CT pulmonary angiography with dual-energy monochromatic imaging: comparison with standard CT pulmonary angiography—a prospective randomised trial. Radiology 262:290–297
2. Shuman WP, Chan KT, Busey JM, Mitsumori LM, Koprowicz KM (2016) Dual-energy CT aortography with 50% reduced iodine dose versus single-energy CT aortography with standard iodine dose. Acad Radiol 23:611–618
3. Agrawal MD, Oliveira GR, Kalva SP, Pinho DF, Arellano RS, Sahani DV (2016) Prospective comparison of reduced-iodine-dose virtual monochromatic imaging dataset from dual-energy CT angiography with standard-iodine-dose single-energy CT angiography for abdominal aortic aneurysm. AJR Am J Roentgenol 207: W125–W132
4. Machida H, Tanaka I, Fukui R et al (2016) Dual-energy spectral CT: various clinical vascular applications. Radiographics 36:1215–1232
5. Chen Y, Zhang X, Xue H et al (2017) Head and neck angiography at 70 kVp with a third-generation dual-source CT system in patients: comparison with 100 kVp. Neuroradiology 59:1071–1081
6. Laimi K, Salminen JJ, Metsahonkala L et al (2007) Characteristics of neck pain associated with adolescent headache. Cephalalgia 27: 1244–1254
7. Jull G, Amiri M, Bullock-Saxton J, Darnell R, Lander C (2007) Cervical musculoskeletal impairment in frequent intermittent headache. Part 1: subjects with single headaches. Cephalalgia 27:793–802
8. Amiri M, Jull G, Bullock-Saxton J, Darnell R, Lander C (2007) Cervical musculoskeletal impairment in frequent intermittent headache. Part 2: subjects with concurrent headache types. Cephalalgia 27:891–898
9. Urrutia J, Besa P, Campos M et al (2016) The Pfirrmann classification of lumbar intervertebral disc degeneration: an independent inter- and intra-observer agreement assessment. Eur Spine J 25: 2728–2733
10. Jones A, Clarke A, Freeman BJ, Lam KS, Grevitt MP (2005) The Modic classification: inter- and intraobserver error in clinical practice. Spine (Phila Pa 1976) 30:1867–1869
11. Marinelli NL, Haughton VM, Munoz A, Anderson PA (2009) T2 relaxation times of intervertebral disc tissue correlated with water content and proteoglycan content. Spine (Phila Pa 1976) 34:520–524
12. Thalgott JS, Albert TJ, Vaccaro AR et al (2004) A new classification system for degenerative disc disease of the lumbar spine based on magnetic resonance imaging, provocative discography, plain radiographs and anatomic considerations. Spine J 4:167S–172S
13. Rizzo S, Radice D, Femia M et al (2018) Metastatic and non-metastatic lymph nodes: quantification and different distribution of iodine uptake assessed by dual-energy CT. Eur Radiol 28:760–769
14. Darras KE, McLaughlin PD, Kang H et al (2016) Virtual monoenergetic reconstruction of contrast-enhanced dual energy CT at 70keV maximizes mural enhancement in acute small bowel obstruction. Eur J Radiol 85:950–956
15. Yang CB, Zhang S, Jia YJ et al (2017) Dual energy spectral CT imaging for the evaluation of small hepatocellular carcinoma microvascular invasion. Eur J Radiol 95:222–227
16. Milette PC (2000) Classification, diagnostic imaging, and imaging characterization of a lumbar herniated disk. Radiol Clin North Am 38:1267–1292
17. Pfirrmann CW, Metzdorf A, Zanetti M, Hodler J, Boos N (2001) Magnetic resonance classification of lumbar intervertebral disc degeneration. Spine (Phila Pa 1976) 26:1873–1878
18. Adams A, Roche O, Mazumder A, Davagnanam I, Mankad K (2014) Imaging of degenerative lumbar intervertebral discs; linking anatomy, pathology and imaging. Postgrad Med J 90:511–519
19. Schueller-Weidekamm C, Schaefer-Prokop CM, Weber M, Herold CJ, Prokop M (2006) CT angiography of pulmonary arteries to detect pulmonary embolism: improvement of vascular enhancement with low kilovoltage settings. Radiology 241:899–907
20. Bonatti M, Lombardo F, Zamboni GA, Pernter P, Pozzi Mucelli R, Bonatti G (2017) Dual-energy CT of the brain: comparison between DECT angiography-derived virtual unenhanced images and true unenhanced images in the detection of intracranial haemorrhage. Eur Radiol 27:2690–2697
21. Marin D, Davis D, Roy Choudhury K et al (2017) Characterization of small focal renal lesions: diagnostic accuracy with single-phase contrast-enhanced dual-energy CT with material attenuation analysis compared with conventional attenuation measurements. Radiology 284:737–747
22. Vergroesen PP, Kingma I, Emanuel KS et al (2015) Mechanics and biology in intervertebral disc degeneration: a vicious circle. Osteoarthr Cartil 23:1057–1070
23. Lotz JC, Haughton V, Boden SD et al (2012) New treatments and imaging strategies in degenerative disease of the intervertebral disks. Radiology 264:6–19
24. Watanabe A, Benneker LM, Boesch C, Watanabe T, Obata T, Anderson SE (2007) Classification of intervertebral disk degeneration with axial T2 mapping. AJR Am J Roentgenol 189:936–942
25. Marinelli NL, Haughton VM, Anderson PA (2010) T2 relaxation times correlated with stage of lumbar intervertebral disk degeneration and patient age. AJNR Am J Neuroradiol 31:1278–1282